Laser Light Scattering Characterization of Molecular Weight Distribution of Worm-Like Chains Poly(1,4-phenylene terephthalamide) in Concentrated Sulfuric Acid*,[1]

BENJAMIN CHU,†‡ CHI WU,† AND JAMES R. FORD†

†*Chemistry Department and* ‡*Department of Materials Science and Engineering, State University of New York at Stony Brook, L. I., N. Y. 11794-3400*

Received October 1, 1984; accepted December 12, 1984

By combining static and dynamic light scattering measurements, we have succeeded in determining the molecular weight distribution of poly(1,4-phenylene terephthalamide) in concentrated sulfuric acid using Laplace inversion of the photoelectron autocorrelation function. The complex method of data analysis can be greatly simplified for on-line monitoring purposes by measuring the difference correlation functions whereby changes of molecular weight and of polydispersity can be detected quantitatively by photon correlation measurements at a fixed scattering angle and finite concentration even for worm-like chains. Effects due to concentration, intramolecular interference, and internal motions can be taken into account in the empirical procedure.

I. INTRODUCTION

Solution properties of PPTA have been investigated by Berry and his co-workers (1, 2). The molecular characterizations of polyamides have often been shown to be difficult to perform because of a variety of experimental difficulties. In a recent series of publications (3–5), we have succeeded in characterizing the molecular weight distribution (MWD) of PPTA in concentrated sulfuric acid by means of laser light scattering. We were able to work out a procedure to characterize worm-like chains in dilute solutions. In addition, we determined the fundamental parameters which could be utilized for a straightforward MWD determination of PPTA dissolved in 96% sulfuric acid and 0.05 M K_2SO_4. The experimental difficulties which we need to overcome can be summarized as follows.

1. PPTA fluoresces with a blue (λ_0 = 448 nm) incident laser beam. The fluorescence could be alleviated using incident radiations of higher wavelengths in the green/red region (e.g., 514.5 or 632.8 nm). In our experiments, we also used a narrow-band interference filter centered at the incident wavelength so that residual effects due to fluorescence were further reduced. Finally, agreement on light scattering results using different incident wavelengths confirmed that we could perform light scattering studies on PPTA in concentrated sulfuric acid.

2. PPTA solution has a reddish tint denoting absorption of light in the visible region. Extinction coefficients at different wavelengths were determined separately using a spectrophotometer. Light scattering intensity measurements at different polymer concentrations were corrected for extinction. Agreement of static and dynamic light scattering results using different incident wavelengths and laser power showed that we could per-

* This paper is dedicated to Dr. Milton Kerker on the occasion of his 65th birthday.

[1] Work supported by the National Science Foundation, Polymers Program (DMR 8314193), and the Petroleum Research Fund, administered by the American Chemical Society.

0021-9797/85 $3.00

form proper light scattering experiments in a weakly absorbing solution.

3. Considerable protonation of PPTA in concentrated sulfuric acid results in the formation of macroions. Possible effects due to long-range electrostatic interactions were considered. Although concentrated sulfuric acid has a relatively high ionic strength, we examined the effects of salt (K_2SO_4) on the molecular weight of PPTA in 96% H_2SO_4. The results suggested that *lowest* and constant molecular weights of PPTA could be established by adding a small amount of K_2SO_4. A slight excess (0.05 M) of K_2SO_4 was then added to 96% H_2SO_4 in subsequent studies. The protonated PPTA was also precipitated by adding water to the PPTA solution. Elemental analysis of precipitated PPTA showed the same chemical composition as the original PPTA, indicating an absence of complex formation with sulfates.

4. Rod-like polymer chains usually exhibit strong interchain interactions including aggregation. The absence of aggregation was investigated by examining the variance of the time correlation function and the intrinsic viscosity of PPTA as a function of water content in concentrated sulfuric acid. Final Laplace inversion of the time correlation function of PPTA in 96% H_2SO_4 and 0.05 M K_2SO_4 showed an absence of bimodality, suggesting that aggregation, if present, was not a major factor in the molecular weight distribution.

5. PPTA solutions were difficult to clarify. In the preliminary studies, we determined the centrifugal acceleration required to remove the dust particles but not the PPTA polymers from solution. We did not filter the PPTA solutions partly because rod-like polymer chains tended to plug up the filter and partly because filters were less effective in removing dust particles from a polar and corrosive solvent, such as concentrated sulfuric acid. The clarified solution was examined for large dust particles using a weak laser beam and a magnifying lens. Final confirmation on solution clarity could be established when the measured baseline agreed with the computed baseline to within ~0.1% in the intensity–intensity time correlation function $G^{(2)}(\tau)$ at different scattering angles.

6. The use of H_2SO_4 + K_2SO_4 + H_2O represents a mixed solvent. Dialysis would have been difficult to perform in view of the corrosive nature of concentrated sulfuric acid to most semipermeable membranes. We could establish the fact that measurements at different concentrations were performed at the same chemical potential because the refractive index increment of PPTA in 96% H_2SO_4 remained unchanged in the presence of varying amounts of K_2SO_4.

7. PPTA is anisotropic. Light scattering intensity measurements using vertically polarized incident and scattered light (vv) optical geometry could yield only apparent molecular weight and radius of gyration. We measured both polarized and depolarized components of scattered light (6) for PPTA in 96% H_2SO_4 + 0.05 M K_2SO_4.

In our analysis, we used $D_0 = k_D M^{-0.75}$ where D_0 and M are expressed in square centimeters per second and gram per mole, respectively, and $k_D = 2.07 \times 10^{-5}$. The empirical relationship (4) between the translational diffusion coefficient at infinite dilution D_0 (actually D_z) and the molecular weight M (actually M_w) was determined using five molecular weight fractions ranging from $M_w = 1.5 \times 10^4$ to $M_w = 4 \times 10^4$ g/mole. Therefore, the exponent ($\alpha_D = 0.75$) represents an effective value for a limited range of molecular weight. Strictly speaking, the exponent should not be a constant over a broad molecular weight range because PPTA has an estimated persistence length of 290 Å which implies rigid-rod behavior with $\alpha_D = 1$ for very-low-molecular weight fractions and polymer coil behavior with $\alpha_D \sim 0.6$ for very-high-molecular-weight fractions, if they exist.

In this article, we wish to report that a simple analytical procedure can be established

to determine the molecular weight and its variance of a PPTA polymer using dynamic light scattering measurements at one scattering angle and one finite concentration without employing the complex Laplace inversion method.

II. BRIEF THEORETICAL REVIEW

II.1. Spectrum of Scattered Light

In the self-beating mode, the measured full photoelectron count autocorrelation function $G^{(2)}(\tau, K)$ for a detector of finite effective photocathode has the form (6)

$$G^{(2)}(\tau, K) = N_s\langle n\rangle^2(1 + b|g^{(1)}(\tau, K)|^2), \quad [1]$$

where $g^{(1)}(\tau, K)$ is the first-order normalized scattered electric field (E_s) time correlation function, τ is the delay time, $\langle n\rangle$ denotes the mean counts per sample time, N_s is the total number of samples, A [$=N_s\langle n\rangle^2$] is the baseline, and b is a spatial coherence factor depending upon experimental conditions and is usually taken as an unknown parameter in the data-fitting procedure. As $\tau \to 0$, $g^{(1)}(0, K) = \langle E_s^*(0, K)E_s(0, K)\rangle \propto R_{vv}(K)$, where $R_{vv}(K)$ is the excess Rayleigh ratio measured at a fixed value of K and $K = (4\pi/\lambda)\sin(\theta/2)$ with λ and θ being the wavelength of light in the scattering medium and the scattering angle, respectively.

For a solution of polydisperse particles (or macromolecules), $g^{(1)}(\tau, K)$ has the form (7)

$$g^{(1)}(\tau, K) = \int_0^\infty G(\Gamma, K)e^{-\Gamma(K)\tau}d\Gamma. \quad [2]$$

As $\tau \to 0$, $g^{(1)}(0, K) = \int_0^\infty G(\Gamma, K)d\Gamma$, where $G(\Gamma, K)$ is the normalized distribution of linewidth Γ measured at a fixed value of K. Thus, $\int_0^\infty G(\Gamma, K)d\Gamma \propto R_{vv}(K)$.

The average linewidth $\bar{\Gamma}$ [$\equiv\int_0^\infty \Gamma G(\Gamma)d\Gamma$] at a finite concentration C can be written as (8)

$$D^*(M, K) = \bar{\Gamma}(M, K)/K^2 = D(M)(1 + f_M\langle R_g^2\rangle_{app}K^2), \quad [3]$$

where $D(M)$ represents the molecular weight dependent translational diffusion coefficient at a finite concentration with

$$D(M) = D_0(M)(1 + k_dC). \quad [4]$$

$D_0(M)$ is the translational diffusion coefficient at infinite dilution. $\langle R_g^2\rangle^{1/2}$ is the apparent root mean square radius of gyration at concentration C without correction for molecular anisotropy. k_d is an average system-specific second virial (diffusion) coefficient. f_M is a dimensionless number which depends on chain structure, polydispersity, and solvent quality and is an experimentally determined quantity in our scaling procedure to be discussed later.

The inversion of Eq. [2] to obtain the linewidth distribution function $G(\Gamma, K)$ has been the subject of considerable attention in the recent literature (7, 9–20). Different techniques, such as singular value decomposition and regularization, yield essentially the same result (5). The details of the singular value decomposition technique have been described elsewhere (17). In this article, we model $G(\Gamma, K)$ as a weighted sum of Dirac delta functions

$$G(\Gamma, K) = \sum_{i=1}^{N} G(\Gamma_i, K)\delta(\ln\Gamma - \ln\Gamma_i), \quad [5]$$

where $G(\Gamma_i, K) = P_i(K)/\Gamma_i$ with $P_i(K)$ being the intensity factor. $G(\Gamma, K)$ [$=\sum_{i=1}^N P_i(K)\delta(\Gamma - \Gamma_i)$] was obtained from the Laplace inversion.

II.2. Intensity of Scattered Light

The Rayleigh ratio R_{vv} for vertically polarized incident and vertically polarized scattered light at a finite concentration C in dilute solution has the form (4, 21)

$$HC/R_{vv}(K) = [1 + \langle R_g^2\rangle_{app}K^2/3]M_{app}^{-1} + 2A_2C, \quad [6]$$

where C [g/ml] is the concentration. H [mole cm^2 g^{-2}] is equal to $4\pi^2n^2(dn/dC)^2/(N_A\lambda_0^4)$ with n, N_A, λ_0, and dn/dC being the refractive index, Avogadro's number, the wavelength *in vacuo*, and the refractive index increment,

respectively. A_2 is the second virial coefficient. After correction for molecular anisotropy, δ,

$$M_w = \frac{M_{app}}{1 + 4\delta^2/5} \quad [7]$$

and

$$\langle R_g^2(C)\rangle = \frac{(1 + 4\delta^2/5)\langle R_g^2\rangle_{app}}{1 - \frac{4\delta}{5} + \frac{4\delta^2}{7}}, \quad [8]$$

where the radius of gyration R_g at infinite dilution is related to the radius of gyration at finite concentration $\langle R_g^2(C)\rangle^{1/2}$ according to

$$R_g^2 = \langle R_g^2(C)\rangle[1 + 2A_2MC/(1 + 4\delta^2/5)]. \quad [9]$$

In identifying $D_i^* = \Gamma_i/K^2$ and $\int G(\Gamma, K)d\Gamma = \int G^+(D^*)dD^*$ with the use of Eqs. [3] and [6] where we have set $D_i^* = D_i(1 + f_M R_{g,app,i}^2 K^2)$, the change of variable from Γ to D^* leads to the relation

$$1/G^+(D_i^*, K) = 1 + (f_M + 1/3)R_{g,app,i}^2 K^2 + O(K^4). \quad [10]$$

The superscript + is used to emphasize the scaling of $G(\Gamma, K)$ such that $\int_0^\infty G^+(D^*, K)dD^* = R_{vv}(K)$. Finally, on the $G(D_0)$ axis, we have

$$G^+(D_{0,i}, K) \propto F_w(M_i)M_iP_i(K), \quad [11]$$

where F_w is proportional to the weight fraction W_i having molecular weight M_i. The transformation of experimental data from static and dynamic measurements to yield MWD is illustrated in Fig. 1.

III. EXPERIMENTAL METHODS

PPTA (sample No. 202) was dissolved in concentrated sulfuric acid (96%) and 0.05 M K_2SO_4. The solvent had been centrifuged at 23,000g for 24 hr in order to remove dust particles. All vessels, such as volumetric flasks, centrifuge tubes, light scattering cells, and pipettes were rendered dust-free by washing in distilled and filtered acetone. The PPTA polymer took 2–3 days for complete dissolution. Then, the polymer solution was centrifuged at 12,100g for 24 hr. We took the middle portion of the centrifuged solution for light scattering measurements. The clarified PPTA polymer solution was centrifuged again at 12,100g for 24 hr before light scattering measurements. The experimental setup and other procedures have been described elsewhere (4, 5).

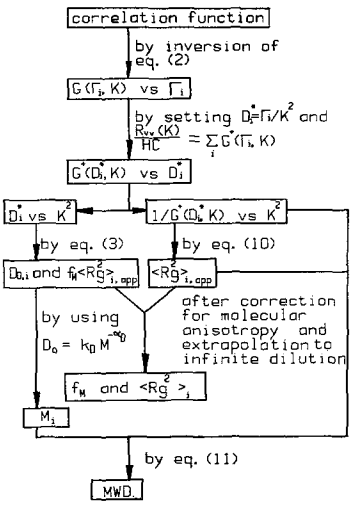

FIG. 1. A schematic flow chart for determination of molecular weight distribution from measurements of time correlation functions $G_{vv}^{(2)}(K, \tau)$ and Rayleigh ratio $R_{vv}(K)$. The subscripts vv denote vertically polarized incident and scattered light.

IV. RESULTS AND DISCUSSION

Figure 2 shows two typical (normalized) partially scaled electric field autocorrelation functions for 5.0×10^{-4} g/ml PPTA ($M_w = 1.35 \times 10^4$ g/mole) in 96% H_2SO_4 and 0.05 M K_2SO_4 at 30°C and $\theta = 30$ and 120°, respectively. For practical convenience, we have set $|g^{(1)}(\Gamma, t = \Delta\tau)| = 1$, not $|g^{(1)}(\Gamma, t = 0)| = 1$ where $\Delta\tau$ is the increment delay time per channel. The partial scaling was achieved by assuming $\Gamma = D^*K^2$. The difference in the two correlation functions after K^2 scaling could be attributed mainly to the presence of internal motions. Therefore, it was essential to use Eq. [3] in order to determine the translational diffusion coefficient D at concentration $C = 5 \times 10^{-4}$ g/ml.

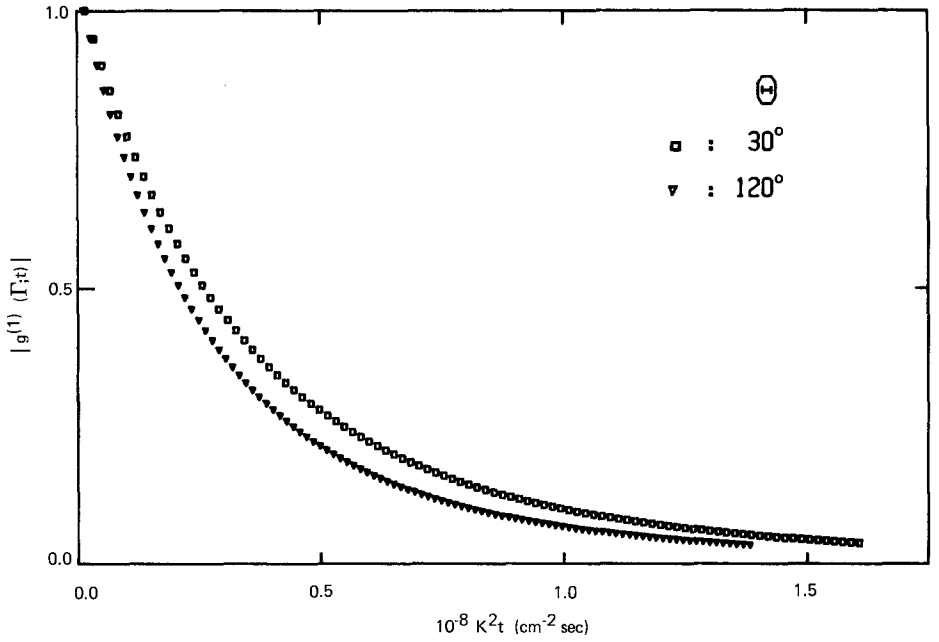

FIG. 2. Typical net (normalized) partially scaled electric field autocorrelation function for 5.0×10^{-4} g/ml PPTA ($M_w = 1.35 \times 10^4$ g/mole) in 96% H_2SO_4 and 0.05 M K_2SO_4 measured at 30°C and $\theta = 30°$ (hollow squares) and 120° (hollow inverted triangles). The difference is due to the presence of internal motions.

Figure 3 shows plots of D_i^* versus K^2 for a few representative fractions, M_i of the MWD. The intercepts yield $D_{0,i}$ and the slopes are related to $(f_M R^2_{g,app,i})$. The uncertainties for $(f_M R^2_{g,app,i})$ are large because of the Laplace inversion and the small slopes. In order to utilize Eq. [10], we must first rescale $\int G(\Gamma, K)d\Gamma = 1$ according to $\int G^+(D^*, K)dD^* = R_{vv}(K)$ as shown in Fig. 4. By setting the integrated scattered intensity at a fixed scattering angle equal to the sum of scattered intensities of the representative fractions at the same scattering angle and by repeating this procedure for different scattering angles, we have rescaled the angular distribution of scattered intensity of each representative fraction. Figure 4 illustrates the observed differences along both the $G^+(D^*)$ axis and the D^* axis as a function of scattering angle. However, it must be noted that the alignment of different representative fractions could introduce substantial errors, especially near the two ends of the $G(\Gamma, K)$ distributions. So, in the Laplace inversion, we were particularly careful to establish a criterion for selecting the end points of the $G(\Gamma, K)$ distributions. Figure 5 shows plots of $1/G^+(D_i^*)$ versus K^2 for a few typical representative fractions. According to Eq. [10], we can determine the apparent radius of gyration, $R^2_{g,app,i}$, at concentration C for each representative fraction. The radius of gyration for some representative fractions at infinite dilution after correction

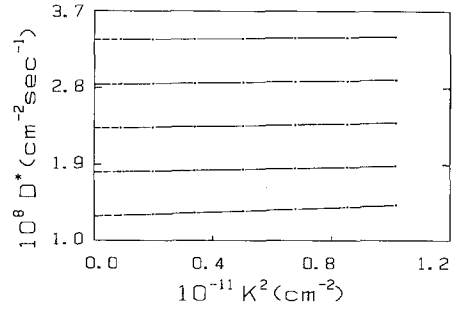

FIG. 3. Plots of selected representative fractions of D^* vs K^2. The results are listed in Table I.

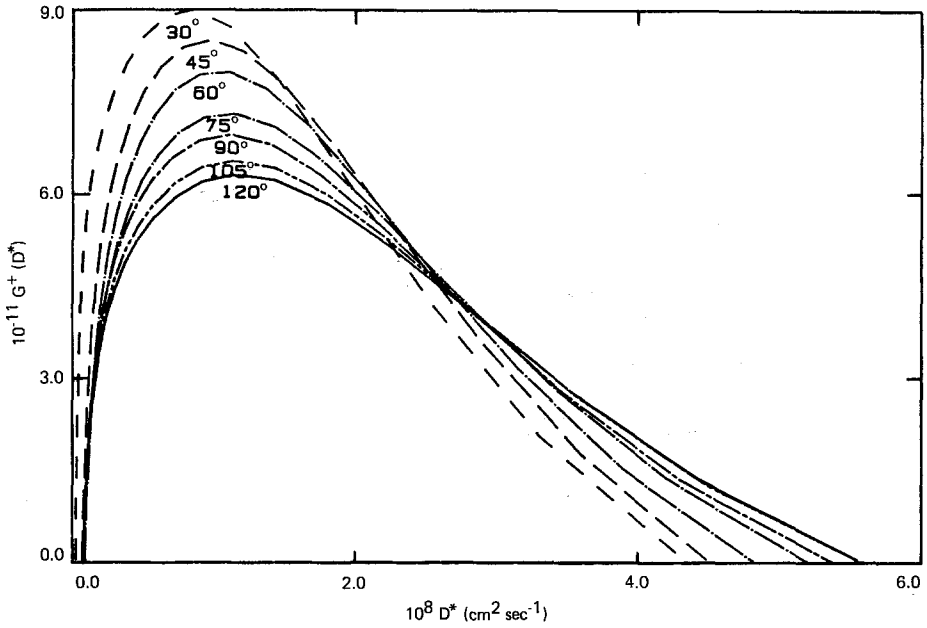

FIG. 4. Plots of $G^+(D^*)$ vs D^* ($\equiv\Gamma/K^2$) for 5×10^{-4} g/ml PPTA ($M_w = 1.35 \times 10^4$ g/mole) in 96% H_2SO_4 and 0.05 M K_2SO_4 measured at 30°C with θ varying from 30 to 120°. $G^+(K, D^*)$ has been scaled such that $\int G^+(K, D^*)dD^* = R_{vv}(k)$.

for molecular anisotropy is listed in Table I. By combining the results of Figs. 3 and 5, we can also have rough estimates for $f(\equiv\bar{f}_M)$at the finite concentration C. Figure 6 shows plots of f (at finite concentrations) versus L/Λ where L [=12.9 M/238 Å with M expressed in g/mole] is the contour length and Λ [$= 2\rho \cong 580$ Å with ρ taken to be 290 Å] is the Kuhn length. Two PPTA fractions with a total of three concentrations are presented.

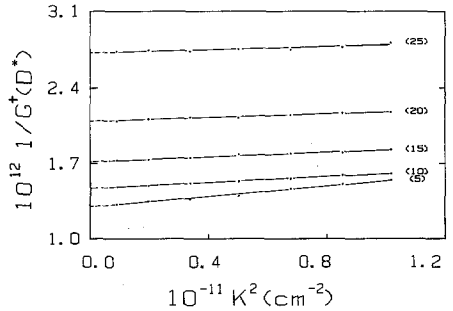

FIG. 5. Plots of selected representative fractions of $1/G^+(D^*, K)$ vs K^2. The results are listed in Table I.

The uncertainties of our results do not permit us to establish f values at infinite dilution. Nevertheless, it is interesting to note that the f values are of reasonable order of magnitude

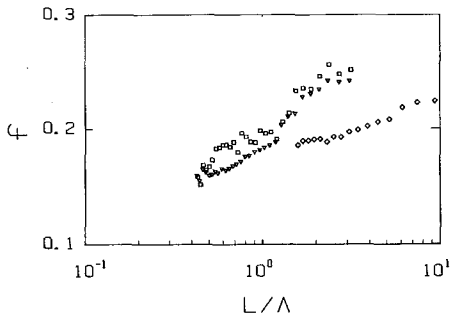

FIG. 6. Plots of f vs L/Λ where L [=12.9 M/238 Å] and Λ are the contour length and the Kuhn length, respectively. $\Lambda = 2\rho = 580$ Å with ρ taken to be 290 Å. $M_w = 4.3 \times 10^4$ g/mole (Ref. (5)), hollow diamonds, $C = 2.8 \times 10^{-4}$ g/mole. $M_w = 1.35 \times 10^4$ g/mole; hollow squares, $C = 5.0 \times 10^{-4}$ g/ml; hollow inverted triangles, $C = 1.7 \times 10^{-4}$ g/ml. f appears to be concentration dependent. In comparison with theory, f should be extrapolated to infinite dilution.

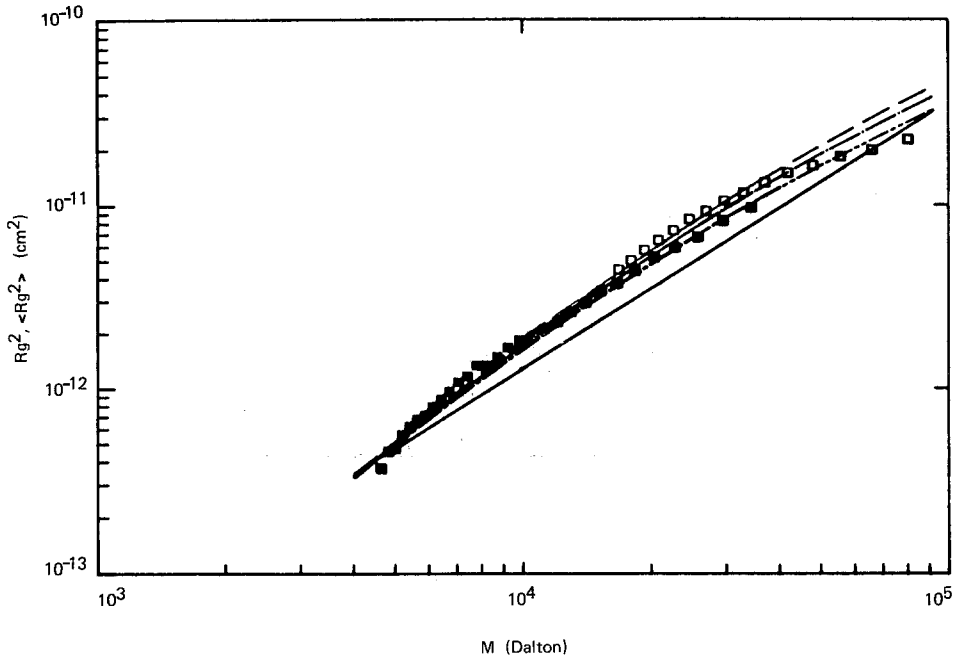

FIG. 7. Plots of $(R_g^2)_i$ vs M_i for representative fractions M_i of the MWD for two PPTA samples with $M_w = 4.3 \times 10^5$ (hollow squares, Ref. (5)) and $M_w = 1.35 \times 10^4$ (filled squares). $\langle R_g^2 \rangle_z$ values for the two PPTA samples of different molecular weights by light scattering intensity measurements fall within the limits of uncertainties of R_g^2 of representative fractions from the two separate samples. Solid line denotes $R_g^2 = 1.22 \times 10^{-18}\ M^{1.5}$ cm^2 with M expressed in g/mole. $R_g^2 = \rho^2[4\rho/3 - 1 + 2/(L/\rho) - [2/(L/\rho)^2](1 - \exp(-L/\rho))]$ with $L = 12.9M/238$ Å (-· ·-) 240 Å, (-···) 290 Å, (---) 340 Å. We estimated $\rho \sim 290$ Å.

TABLE I

Molecular Parameters of Some PPTA-202 Representative Fractions Based on Figs. 3–5

No. of fraction	$D \times 10^8$ (cm^2 sec^{-1})	$M \times 10^{-4}$ (Da)	$R_g^2 \times 10^{12}$ (cm^2)	f
1	0.853	3.39	9.7	0.25
2	1.16	2.26	5.9	0.25
3	1.46	1.65	3.8	0.23
4	1.76	1.28	2.6	0.19
5	2.07	1.04	1.9	0.20
6	2.37	0.865	1.5	0.19
7	2.68	0.736	1.2	0.19
8	2.98	0.638	0.88	0.19
9	3.29	0.560	0.68	0.17
10	3.59	0.498	0.48	0.17

Note. R_g is the radius of gyration at infinite dilution after correction for molecular anisotropy

$$R_{g,i} = \frac{(1 + 4\delta^2/5)}{1 - \frac{4\delta}{5} + \frac{4\delta^2}{7}} [1 + 2A_2MC/(1 + 4\delta^2/5)]R^2_{g,app,i},$$

where A_2 and δ are the average second virial coefficient and molecular anisotropy, respectively.

and increase in a similar fashion as predicted by theory (8). It also appears that f at infinite dilution is likely to be lower than f at finite concentrations. Figure 7 shows plots of radius of gyration R_g^2 as a function of molecular weight of the representative fractions based on values of R_g^2 following the procedure in Fig. 1. If we take $\alpha_R = 0.75$, $R_g^2 \propto M^{1.5}$ as shown by the solid line in Fig. 7. The relation $R_g^2 \propto M^{1.5}$ is only partially valid. For worm-like chains, the exponents α_D and α_R are not really constants because for short worm-like chains, the value of exponents increases toward the rigid-rod limit while for long worm-like chains, the value decreases toward the coil limit. If we take $R_g^2 = \rho^2\{L\rho - 1 + 2/(L/\rho) - [2/(L/\rho)^2](1 - \exp(-(L/\rho))\}$ with ρ ranging from 240 to 340 Å and $L = 12.9\ M/238$ Å, the experimental results are in excellent agreement with theory as shown in Fig. 7. We estimated $\rho = 290 \pm 50$ Å.

Figure 8 shows the molecular weight distributions of two PPTA fractions with $M_w = 1.35 \times 10^4$ and 4.3×10^4 g/mole. The MWD distribution functions were constructed according to the representative fractions and were therefore discrete distributions. In our procedure for transforming $g^{(1)}(\tau)$ to molecular weight distribution, we need to have a good understanding of the ill-conditioned Laplace inversion problem which is likely to be beyond the common knowledge needed in a polymer chemical laboratory. Furthermore, for polycondensation polymers with $D_0 \propto M^{-0.75}$, the variance of the linewidth distribution, $\mu_2/\bar{\Gamma}^2$ (with $\mu_2 = \int G(\Gamma)(\Gamma - \bar{\Gamma})^2 d\Gamma$), is likely to be broad. Then, the cumulants method (22) of data analysis yields imprecise values for the width of $G(\Gamma)$ because one does not know the number of terms in the cumulants expansion needed to determine a correct μ_2. An alternative procedure has been proposed (23). In the cumulants expansion

$$\ln|g^{(1)}(t)| = -\bar{\Gamma}t + \tfrac{1}{2}\mu_2 t^2 + \cdots. \quad [12]$$

The difference term can then be represented by

$$\ln|g_1^{(1)}(t)| - \ln|g_2^{(1)}(t)| = -(\bar{\Gamma}_1 - \bar{\Gamma}_2)t + \tfrac{1}{2}(\mu_{2,1} - \mu_{2,2})t^2 - \cdots. \quad [13]$$

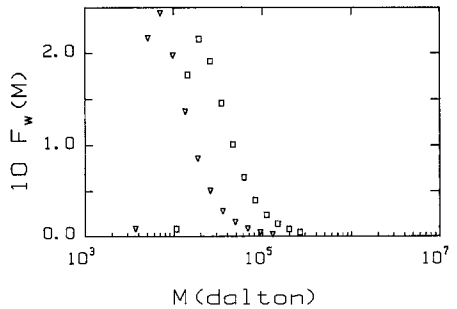

FIG. 8. Molecular weight distributions of PPTA fractions. $M_w = 4.3 \times 10^4$ g/mole (Ref. (5)), hollow squares, $M_w = 1.35 \times 10^4$ g/mole (M_z:M_w:$M_n \geq$ 5.3:1.57:1), hollow diamonds.

By combining Eqs. [3], [4], and [13], we get

$$\ln|g_1^{(1)}(t, C_1)| - \ln|g_2^{(2)}(t, C_2)| = -[\bar{D}_{0,1}(1 + k_d C_1)(1 + f_M\langle R_g^2\rangle_{app,1}K^2)K^2 - \bar{D}_{0,2}(1 + k_d C_2)(1 + f_M\langle R_g^2\rangle_{app,2}K^2)K^2]t + \tfrac{1}{2}(\mu_{2,1} - \mu_{2,2})t^2 - \cdots. \quad [14]$$

According to Eq. [14], if we know k_d and the concentrations, the concentration effect can easily be taken into account. The $f_M\langle R_g^2\rangle_{app}K^2$ term is relatively small. Thus, we can use an average $f\langle R_g^2\rangle_{app}$ for all molecular weight fractions which are not too far apart. In a plot of $\log|g_{M_1}^{(1)}(\Gamma, t^*)| - \log|g_{M_2}^{(1)}(\Gamma, t^*)|$ versus t^* [$=tK^2(1 + f\langle R_g^2\rangle K^2)$], as shown in Fig. 9, we have

$$\log|g_{M_1}^{(1)}(\Gamma, t^*)| - \log|g_{M_2}^{(1)}(\Gamma, t^*) = \frac{1}{-(2.303)}[\bar{D}_{0,1}(1 + k_d C_1) - \bar{D}_{0,2}(1 + k_d C_2)]t^* + \frac{1}{(2.303 \times 2)}(\bar{D}_{2,1} - \bar{D}_{2,2})t^{*2}, \quad [15]$$

where the first term corresponding to the initial slope in the plot is related to the difference of the z-average diffusion coefficient. By least-squares fitting of the difference curve to second-order, we get $\bar{D}_{575} - \bar{D}_{202} = -(8.6 \pm 0.6) \times 10^{-9}$ cm^2/sec and $\bar{D}_{2,575} - \bar{D}_{2,202} = -(7.0 \pm 0.7) \times 10^{-17}$ cm^4/sec^2.

In Fig. 9, we have also plotted the scaled PPTA-575 ($M_w = 4.3 \times 10^4$ g/mole) measured at three scattering angles with $\theta = 45°$ (hollow squares), 90° (hollow inverted triangles), and 129° (hollow diamonds) and the scaled PPTA-202 ($M_w = 1.35 \times 10^4$ g/mole) measured at $\theta = 30°$ (crosses) and 120° (⊡) using values of $f\langle R_g^2\rangle_{app} \sim 2 \times 1 \times 10^{-12}$. It is important to note that in dilute solutions we can always take the concentration effect into account according to Eq. [4], and at small scattering angles, the approximation to use an average $f\langle R_g^2\rangle_{app}$ for a specific polymer system is quite acceptable. The difference curve will yield a straightforward value for

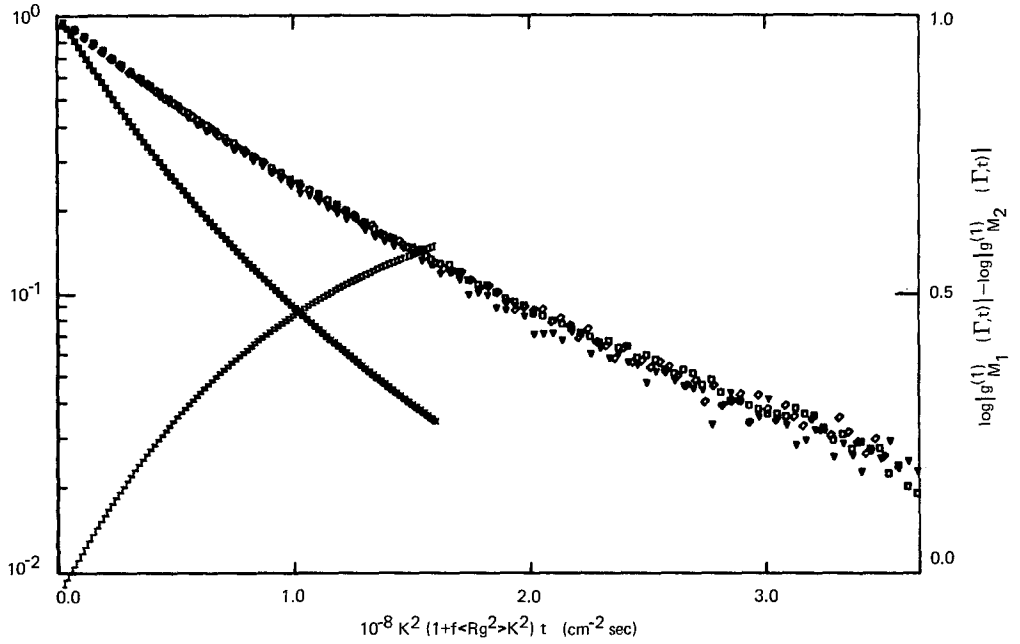

FIG. 9. Scaling of $|g^{(1)}(\Gamma, t)|$ due to interference effect at different concentrations and molecular weights.

Fraction	C (g/ml)	M_w (g/mole)	f	$\langle R_g^2 \rangle_{app}$ (cm^2)
PPTA-202	5×10^{-4}	1.35×10^4	0.18	2.1×10^{-12}
PPTA-575	2.8×10^{-4}	4.3×10^4	0.20	1.2×10^{-11}

PPTA in 96% H_2SO_4 + 0.05 M K_2SO_4 at 30°C. PPTA-575 (□) θ = 45°; (▽) 90°; (◇) 129°. PPTA-202 (×) 30°; (⊡) 120°. Also shown is the difference curve (I, $\log|g^{(1)}_{M_1}(\Gamma, t)| - \log|g^{(1)}_{M_2}(\Gamma, t)|$ for the two PPTA samples.

the $\bar{D}$ difference and a width parameter based on the curvature in the difference plot. For PPTA-575 we have $\bar{D}_{575} = (6.5 \pm 0.5) \times 10^{-9}$ cm^2/sec and $D_{2,575} = (1.2 \pm 0.1) \times 10^{-17}$ cm^2/sec. Similarly, for PPTA-202, we have $\bar{D}_{202} = (1.51 \pm 0.11) \times 10^{-8}$ cm^2/sec and $\bar{D}_{2,202} = (8.2 \pm 0.8) \times 10^{-17}$ cm^4/sec. Both the z-average diffusion coefficient $\bar{D}$ and the second moment of the translational diffusion coefficient $\bar{D}_2$ are often difficult to determine for broad distributions. Parameters for the difference curve are easy to compute according to Eq. [15]. From the Laplace inversion, we get $\bar{D}_{575} - \bar{D}_{202} = -(0.87 \pm 0.05) \times 10^{-8}$ cm^2/sec, in excellent agreement with the result from the difference curve which yields $\bar{D}_{575} - \bar{D}_{202} = -(0.86 \pm 0.06) \times 10^{-8}$ cm^2/sec.

After correction for the concentration effect, $D_{0,202} = (1.5 \pm 0.1) \times 10^{-8}$ cm^2/sec yielding $M_{w,202} \simeq 1.4 \times 10^4$ g/mole in excellent agreement with the result ($M_w \simeq 1.35 \times 10^4$ g/mole) from a much more detailed analysis. For the two PPTA fractions, the diffusion polydispersity parameter $\bar{D}_2/\bar{D}^2 = 0.29 \pm 0.03$ and 0.36 ± 0.05 for PPTA-575 and PPTA-202, respectively. Thus, $\bar{D}_{2,575} - \bar{D}_{2,202}$ should be negative as shown by the result above. In making the difference plot, if we start with a master curve, we can determine changes of the molecular weight average and its polydispersity by making linewidth measurements at one scattering angle and one finite concentration without complex mathematics.

REFERENCES

1. Wong, C.-P., Ohnema, H., and Berry, G. C., *J. Polym. Sci. Polym. Symp.* **65,** 173 (1978).
2. Metzger-Cotts, P., and Berry, G. C., *J. Polym. Sci. Polym. Phys. Ed.* **21,** 1255 (1983).
3. Chu, B., Ying, Q.-C., Wu, C., Ford, J. R., Dhadwal, H., Qian, R.-Y., Bao, J.-S., Zhang, J.-Y., and Xu, C.-C., *Polym. Commun. (Peking)* **25,** 211 (1984).
4. Ying, Q., Chu, B., Qian, R., Bao, J., Zhang, J., and Xu, C., *Polymer,* in press.
5. Chu, B., Ying, Q., Wu, C., Ford, J. R., and Dhadwal, H. S., *Polymer,* in press.
6. Chu, B., "Laser Light Scattering," Chap. 6. Academic Press, New York, 1974.
7. Chu, B., *in* "Proceedings of NATO ASI on the Application of Laser Light Scattering to the Study of Biological Motions" (J. C. Earnshaw and M. W. Steer, Eds.), pp. 53–76. Plenum, New York, 1983.
8. Stockmayer, W. H., and Schmidt, M., *Pure Appl. Chem.* **54,** 407 (1982); *Macromolecules* **17,** 509 (1984).
9. Chu, B., Gulari, Es., and Gulari, Er., *Phys. Scr.* **19,** 476 (1979).
10. McWhirter, J. G., and Pike, E. R., *J. Phys. A: Math. Gen.* **11,** 1729 (1978).
11. Ostrowski, N., Sornette, D., Parker, P., and Pike, E. R., *Opt. Acta* **28,** 1059 (1981).
12. Pike, E. R., *in* "Scattering Techniques Applied to Supramolecular and Non-Equilibrium Systems" (S. H. Chen, B. Chu, and R. Nossal, Eds.), pp. 179–200. Plenum, New York, 1981.
13. Bertero, M., Boccacci, P., and Pike, E. R., *Proc. R. Soc. London Ser. A* **383,** 15 (1982).
14. Stock, G. B., *Biophys. J.* **16,** 535 (1976); **18,** 79 (1978).
15. Provencher, S. W., *Biophys. J.* **16,** 27 (1976); *J. Chem. Phys.* **64,** 2772 (1976); *Makromol. Chem.* **180,** 201 (1979).
16. Provencher, S. W., Hendrix, J., DeMaeyer, L., and Paulussen, N., *J. Chem. Phys.* **69,** 4273 (1978).
17. Ford, J. R., and Chu, B., *in* "Proceedings, 5th International Conference on Photon Correlation Techniques in Fluid Mechanics" (E. O. Schulz-DuBois, Ed.), Springer Series in Optical Sciences, pp. 303–314. Springer-Verlag, New York, 1983.
18. Dahneke, B. E., Ed., "Measurement of Suspended Particles by Quasi-Elastic Light Scattering," pp. 81–252. Wiley, New York, 1983.
19. Schulz-DuBois, E. O., Ed., "Proceedings, 5th International Conference on Photon Correlation Techniques in Fluid Mechanics," Springer Series in Optical Sciences, pp. 286–302, 315–334. Springer-Verlag, New York, 1983.
20. Bertero, M., Boccacci, P., and Pike, E. R., *Proc. R. Soc. London Ser. A* **383,** 15 (1982).
21. Huglin, M. B., *Top. Curr. Chem.* **77,** 143 (1978).
22. Koppel, D. E., *J. Chem. Phys.* **57,** 4814 (1972).
23. Gulari, Er., Gulari, Es., Tsunashima, Y., and Chu, B., *Polymer* **20,** 347 (1979).